



The glacial geomorphology of the Mackenzie Mountains region, Canada

Benjamin J. Stoker, Martin Margold & Duane Froese

To cite this article: Benjamin J. Stoker, Martin Margold & Duane Froese (2023) The glacial geomorphology of the Mackenzie Mountains region, Canada, Journal of Maps, 19:1, 2203333, DOI: [10.1080/17445647.2023.2203333](https://doi.org/10.1080/17445647.2023.2203333)

To link to this article: <https://doi.org/10.1080/17445647.2023.2203333>



© 2023 The Author(s). Published by Informa UK Limited, trading as Taylor & Francis Group on behalf of Journal of Maps



[View supplementary material](#)



Published online: 20 Apr 2023.



[Submit your article to this journal](#)



Article views: 1168



[View related articles](#)



[View Crossmark data](#)



The glacial geomorphology of the Mackenzie Mountains region, Canada

Benjamin J. Stoker^a, Martin Margold^a and Duane Froese^b

^aDepartment of Physical Geography and Geoecology, Charles University, Prague, Czechia; ^bDepartment of Earth and Atmospheric Sciences, University of Alberta, Edmonton, Canada

ABSTRACT

During the Last Glacial Maximum, the Mackenzie Mountains region was glaciated by three distinct ice sources; the Laurentide Ice Sheet, the Cordilleran Ice Sheet, and independent montane glaciers. Rapid ice sheet thinning of the Laurentide-Cordilleran ice saddle in the south of this region contributed to rapid sea level rise events and influenced the style of deglaciation to the north. The current understanding of the glacial history of the broader region has been established through mapping from aerial imagery and early surveys between the early 1970s to the 2010s. The central portions of the Mackenzie Mountains have not yet been mapped. We present a new glacial geomorphological map for the Mackenzie Mountains region covering over 220,000 km². This updated geomorphological map will form the basis of future work to reconstruct the former maximum ice extents, flow dynamics, and retreat pattern.

ARTICLE HISTORY

Received 20 August 2021

Revised 5 March 2023

Accepted 5 April 2023

KEYWORDS

Glacial geomorphology;
Laurentide Ice Sheet; remote
sensing

1. Introduction

Recent numerical modelling studies have identified the northwest Laurentide Ice Sheet (LIS) as a significant contributor to the Meltwater Pulse-1a sea level rise event (Gregoire et al., 2012; Gregoire et al., 2016; Menounos et al., 2017). The collapse of the saddle between the NW LIS and the Cordilleran Ice Sheet (CIS) provides a mechanism to understand the rapid retreat of this ice sheet sector and its contribution to sea level rise (Gomez et al., 2015; Stoker et al., 2022). Improved empirical constraints on the maximum ice extent, flow dynamics, and retreat pattern will allow us to better understand the drivers of rapid ice sheet retreat.

The current ice margin reconstruction of the Mackenzie Mountains and adjacent Mackenzie Valley is based on field surveys and mapping from aerial photographs since the 1970s. This began with work in the early 1970s by Rutter et al. (1993) during the original proposal for the Mackenzie Valley Pipeline and continued to the 2010s (Figure 1) (Boydell & Rutter, 1980; Duk-Rodkin, 2001a, 2001b, 2001c, 2001d, 2001e, 2001f, 2002, 2005, 2009a, 2009b, 2018; Duk-Rodkin & Hughes, 1993a, 1993b, 1995, 2002; Duk-Rodkin & Huntley, 2018a, 2018b; Dyke, 1990a, 1990b, 1990c, 1990d; Turner et al., 2008a). These studies mapped the surficial geology at a range of scales from 1:50,000 to 1:250,000. Directly to the south of the study region, the surficial geology of the Liard region was mapped at 1:50,000 and 1:100,000

scale (e.g. Bednarski, 2008a; Smith, 2003a, 2003b). A series of compilation or broad-scale maps have also been published, covering parts of the study region, largely focusing on the Mackenzie Corridor (Brown et al., 2011; Dalton et al., 2020; Duk-Rodkin, 1999, 2022; Duk-Rodkin et al., 1996, 2004; Dyke et al., 2003; Rutter et al., 1993; Shaw et al., 2010a, 2010b).

The Mackenzie Mountains were glaciated by three distinct ice sources during the local Last Glacial Maximum. The LIS abutted the Canyon Ranges, which form the eastern mountain front of the Mackenzie Mountains, and extended almost 50 km west up the major valleys (Figure 1) (Duk-Rodkin & Hughes, 1991). The CIS advanced from the southwest, through the valleys and into the Backbone Ranges of the central Mackenzie Mountains (Figure 1) (Duk-Rodkin & Hughes, 1991). Finally, independent montane glaciers grew in the Backbone Ranges and contributed to the CIS, acting as an accumulation zone (Turner et al., 2008a, 2008b). The geomorphological record documents the interaction and relative patterns of advance and retreat of these ice masses during the last glaciation. In multiple locations, landforms from montane glaciers are clearly cross-cut by landforms from the LIS (Duk-Rodkin & Hughes, 1991). In the Liard region, to the south of our study area, the deflection of glacially streamlined landforms indicates the coalescence of the LIS and CIS (Bednarski, 2008b; Margold et al., 2013; Smith, 2003a, 2003b). Cross-

CONTACT Benjamin J. Stoker ✉ ben.stoker18@hotmail.com 📧 Department of Physical Geography and Geoecology, Charles University, Prague 128 43, Czechia

📄 Supplemental map for this article is available online at <https://doi.org/10.1080/17445647.2023.2203333>.

© 2023 The Author(s). Published by Informa UK Limited, trading as Taylor & Francis Group on behalf of Journal of Maps

This is an Open Access article distributed under the terms of the Creative Commons Attribution License (<http://creativecommons.org/licenses/by/4.0/>), which permits unrestricted use, distribution, and reproduction in any medium, provided the original work is properly cited. The terms on which this article has been published allow the posting of the Accepted Manuscript in a repository by the author(s) or with their consent.

cutting relationships indicate an early advance of the LIS into the lower valleys of the region, followed by coalescence and buttressing with the CIS, which allowed the ice sheets to thicken and overtop the mountain summits (Smith, 2003a, 2003b).

The Mackenzie Mountains have experienced multiple cycles of glaciation of variable extents (Duk-Rodkin & Barendregt, 2011; Duk-Rodkin & Hughes, 1992). Duk-Rodkin and Hughes (1992) suggested that the penultimate montane and CIS glaciation, which they term the Mountain River glaciation, was the most extensive. They correlate this glaciation with the Reid glaciation of the CIS in neighbouring Yukon. They suggest the last glaciation was less extensive and term it the Gayna River glaciation, correlated with McConnell glaciation (Duk-Rodkin et al., 1996; Duk-Rodkin & Hughes, 1992). These age classifications are based on moraine morphology, palaeosol development, and magnetostratigraphy, with no numerical dating constraints to differentiate the exact timing of these glaciations (Duk-Rodkin et al., 2004; Duk-Rodkin & Hughes, 1992; Trommelen & Levson, 2008). In contrast, the LIS only extended into the North American Cordillera during the last glaciation and so was most extensive in the Mackenzie Mountains region during the Last Glacial Maximum (Duk-Rodkin et al., 1996; Jackson et al., 2011; Zazula et al., 2004).

The development of remote sensing methods and the increase in freely-available, high-resolution digital elevation models provides an opportunity to revisit the geomorphology of the Mackenzie Mountains region. In particular, the ArcticDEM provides an advantage in visualising low-relief and large-scale features. We present a new glacial geomorphological map which complements the pre-existing surficial geology maps and provides robust, empirical evidence for future studies to reconstruct the glacial history of this region.

2. Methods

2.1. Data usage and mapping procedure

The map area covers a total of $\sim 220,000$ km², encompassing 21 1:250,000 map sheet areas (Figure 1). When referring to the mapped area, we use the term ‘Mackenzie Mountains region’ as our map area includes the foothills and Mackenzie Valley to the east. The mapping extent was designed to cover the area of maximum ice margin positions in the Mackenzie Mountains and central area of montane glaciation. Two primary data sources were used in the creation of the glacial geomorphological map. Mapping was performed principally on the 2 m resolution ArcticDEM elevation dataset (Porter et al., 2018). A hillshade relief model was created within ArcMap v10.6.1 from the ArcticDEM dataset to enhance landform visibility. To prevent any mapping errors from

the direction of illumination, we created multiple hillshaded elevation models with different azimuth angles and illumination altitudes (Smith & Clark, 2005). This includes hillshades with an azimuth angle of 315° and 45° and illumination altitudes of 20 and 45. These hillshades were then overlain by a semi-transparent elevation layer. Where the ArcticDEM was not available due to data gaps or poor quality data, satellite imagery at a resolution of 5 m from PlanetLabs was used (Planet Team, 2018). Geomorphological mapping from satellite imagery was limited by image availability and poor lighting conditions, so in these areas only the largest landforms have been mapped. We followed the recommended methodology for the mapping of glacial geomorphology as described in Chandler et al. (2018). To maximise the reliability of the mapping procedure, a repeat-pass method was adopted where each map tile was mapped multiple times with a set scale of 1:25,000–1:50,000.

Secondary mapping datasets were used to supplement the primary data and reduce the misinterpretation of landforms where available. Our final geomorphological map was compared to existing surficial geological maps from the region to evaluate the limitations of our mapping process and identify where new information and understanding has been added. The coverage of pre-existing surficial geology maps across the study region is not complete. Therefore, we only include landforms from the surficial geology maps which are visible in the remote sensing data sources we used to ensure consistency across the study region. Discrepancies between our geomorphological map and pre-existing surficial maps are highlighted throughout the results section.

2.2. Map units

In the following section, we briefly define the landforms mapped, their formative mechanisms, and their potential use for palaeoglaciological reconstruction. We explain the procedure for digitising each map unit and provide examples to illustrate some of the mapped landforms.

2.2.1. Glacial lineations

Glacial lineations are elongate, linear ridges formed by basal sliding of ice masses and/or the deformation of subglacial sediments (e.g. till). We include all ice-flow parallel subglacial bedforms (streamlined bedrock, drumlins, mega-scale glacial lineations, flutings, crag and tails) in the category of glacial lineations. There is debate about the precise processes responsible for the formation of glacial lineations (Clark et al., 2003; Ely et al., 2016; Fowler, 2000; Möller & Dowling, 2018; Stokes et al., 2013), and these features may form through a variety of erosional and/or depositional processes (Eyles et al., 2016; Hart et al.,

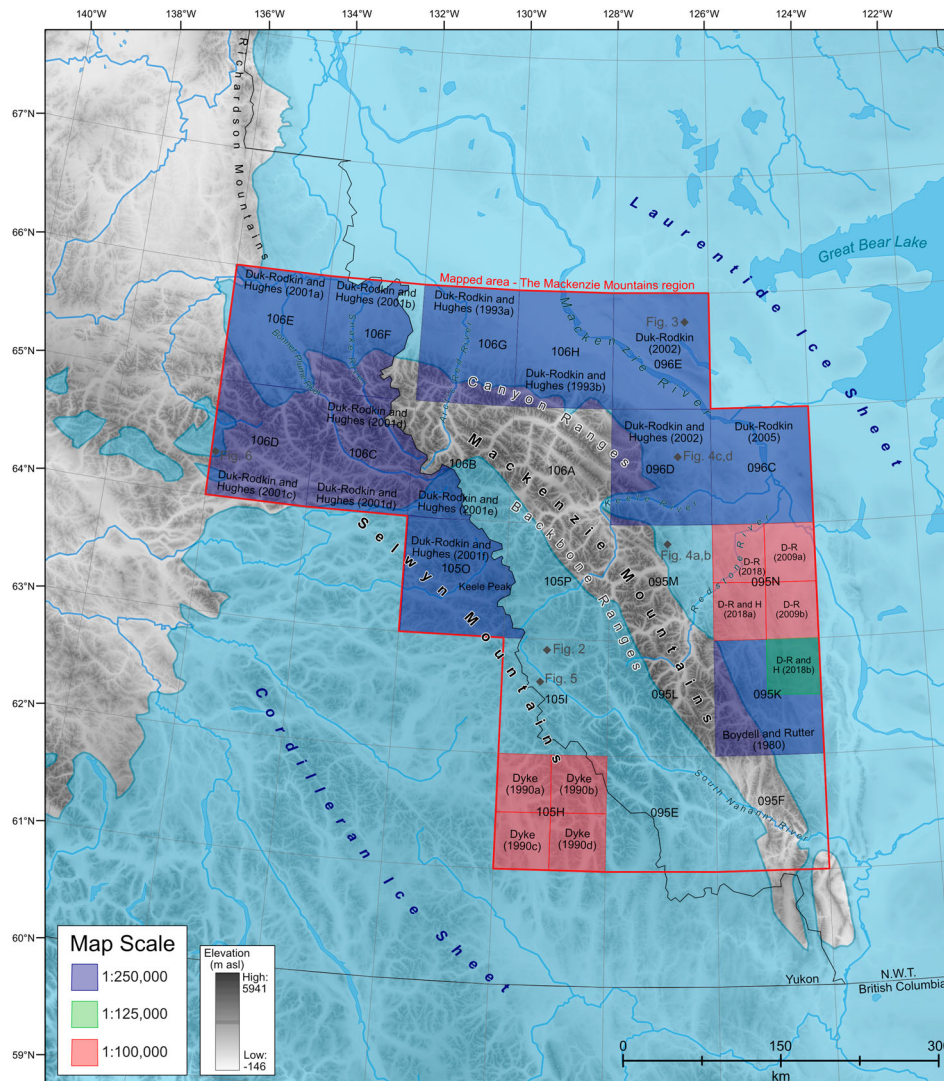


Figure 1. Location map of the Mackenzie Mountains region, Northwest Territories and Yukon. Reconstructed former glacial limits from Dalton et al. (2020) are shown by the blue shaded area. The NTS tiles mapped in this study are labelled in black text. Grey diamonds indicate the location of the figures within this paper. In tile 095N and 095 K/NE, D-R = Duk-Rodkin and H = Huntley.

2018). Glacial lineations can be used to reconstruct the variations in palaeo-ice flow directions. The elongation of glacial lineations has been hypothesised to reflect the ice flow velocity they were formed under, with mega-scale glacial lineations also being diagnostic of former ice stream positions (King et al., 2009; Stokes & Clark, 2002). We mapped all glacial lineations as polylines along the crestline (Figure 2) and in the Main Map we provide arrows to indicate the former ice flow direction alongside swarms of glacial lineations.

2.2.2. Meltwater channels

Meltwater channels are carved by drainage of meltwater from ice sheets and glaciers. They can form in a variety of locations relative to ice masses. We have divided meltwater channels into: lateral (marginal and submarginal) meltwater channels, based on the diagnostic criteria of Greenwood et al. (2007), undifferentiated meltwater channels, and lateral meltwater spillways.

2.2.2.1. Lateral meltwater channels. Lateral meltwater channels are eroded by meltwater flow concentrated between the margin of an ice mass and the local topography. Typically, they form as a series of subparallel channels which are subparallel to contour lines and are discordant with the contemporary drainage network (Greenwood et al., 2007). They commonly appear perched on valley slopes with an abrupt initiation and termination and may be associated with kame terraces and deltas (Figure 4). We have grouped both submarginal and marginal channels into one landform assemblage of lateral meltwater channels due to the fact they both form near to the ice margin. Both submarginal and marginal channels are indicators of ice retreat direction and margin location and have similar characteristics which can make them difficult to distinguish from each other (Kleman, 1992). We mapped all lateral meltwater channels as polylines along the channel thalweg (Figure 4a and 4b); an arrow is provided alongside each

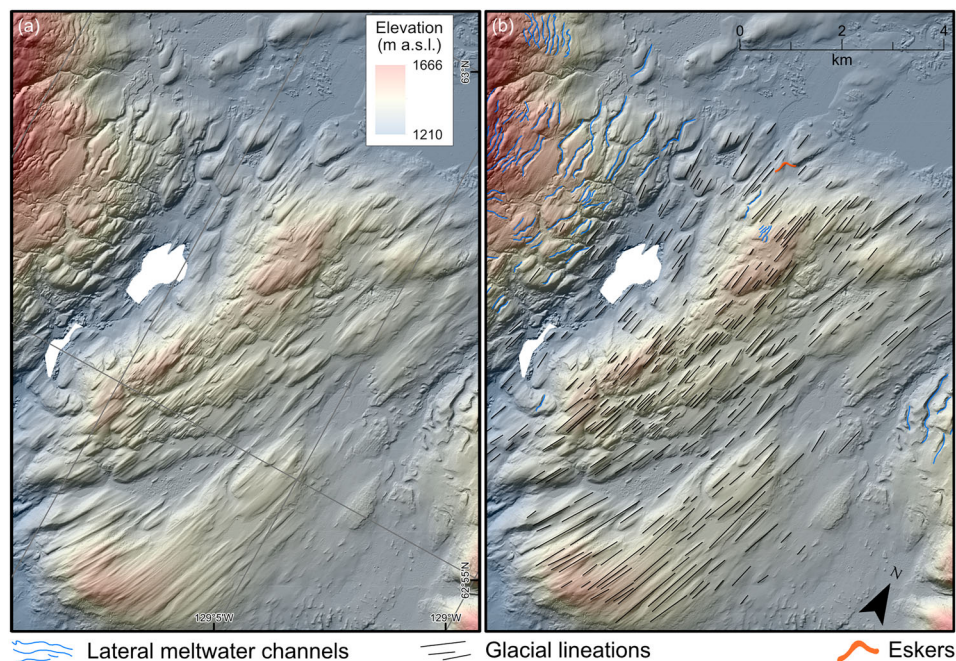


Figure 2. A hillshade image overlain by elevation data from the ArcticDEM showing glacial lineations in the western Mackenzie Mountains. Image location is shown in Figure 1. (a) Closely-spaced lineations in a valley bottom, glacial lineations are especially pronounced on bedrock outcrops. (b) The associated geomorphological mapping of glacial landforms.

swarm of lateral meltwater channels to indicate the former meltwater flow direction. We place lateral meltwater channels into four categories based on the ice source they formed from: Laurentide, Cordilleran, montane, and unknown origin.

2.2.2.2. *Undifferentiated meltwater channels.*

Undifferentiated meltwater channels may include all types of channels formed by the drainage of meltwater. This includes: subglacial meltwater channels, proglacial meltwater channels, and some lateral meltwater channels. Subglacial meltwater channels and tunnel valleys are the erosional product of channelised drainage beneath an ice sheet or glacier (Ó Cofaigh, 1996; Shreve, 1972). Subglacial meltwater channels can be part of a larger chaotic network of bifurcating channels or of single channel systems cutting through topography (Sugden et al., 1991). Proglacial meltwater channels are channels formed by the drainage of meltwater, which may cut across interfluves, drain along established fluvial networks, or establish new drainage channels as water flows freely away from the ice margin. In this category, we include: glacial lake spillways, proglacial drainage channels (Greenwood et al., 2007) and over-col spillways (Margold & Jansson, 2012).

Differentiating between different types of meltwater channels can be difficult, especially in areas of low topographic relief. To avoid any misclassification we group subglacial and proglacial meltwater channels into one landform group. The majority of lateral meltwater channels are included in a separate category, but some may be included in this category. We separate undifferentiated meltwater channels into two size

categories in our map. We define small undifferentiated channels as less than 1000 m wide and map them as polylines along the channel thalweg. We map large undifferentiated meltwater channels (>1000 m wide) as polygons along the break of slope between the channel base and channel walls, as can be seen in Figure 3.

2.2.2.3. *Lateral meltwater spillways.*

As the northwest LIS advanced to the eastern front range of the Mackenzie Mountains it blocked the regional eastward drainage (Bednarski, 2008a, 2008b; Lemmen et al., 1994; Matthews, 1980). During deglaciation, a series of glacial lakes formed between the retreating LIS margin and the Mackenzie Mountains. The regional ice sheet configuration meant that the drainage of these lakes was forced northwards, broadly following the former ice sheet margin, resulting in right-angle diversions of the easterly drainage routes. This south–north oriented drainage carved a series of lateral meltwater spillways along the range front of the Mackenzie Mountains which cut across the interfluves. We map these lateral meltwater spillways as a separate feature as they can provide an insight into the former ice sheet margin configuration and the drainage of glacial lakes. Lateral meltwater spillways are mapped as polygons along the channel base (Figure 4c and 4d).

2.2.3. *Eskers*

Eskers are sinuous ridges of glaciofluvial sands and gravels that are most commonly deposited within conduits at the glacier bed (Brennand, 2000; Storrar et al., 2014). Esker morphology can be highly variable,

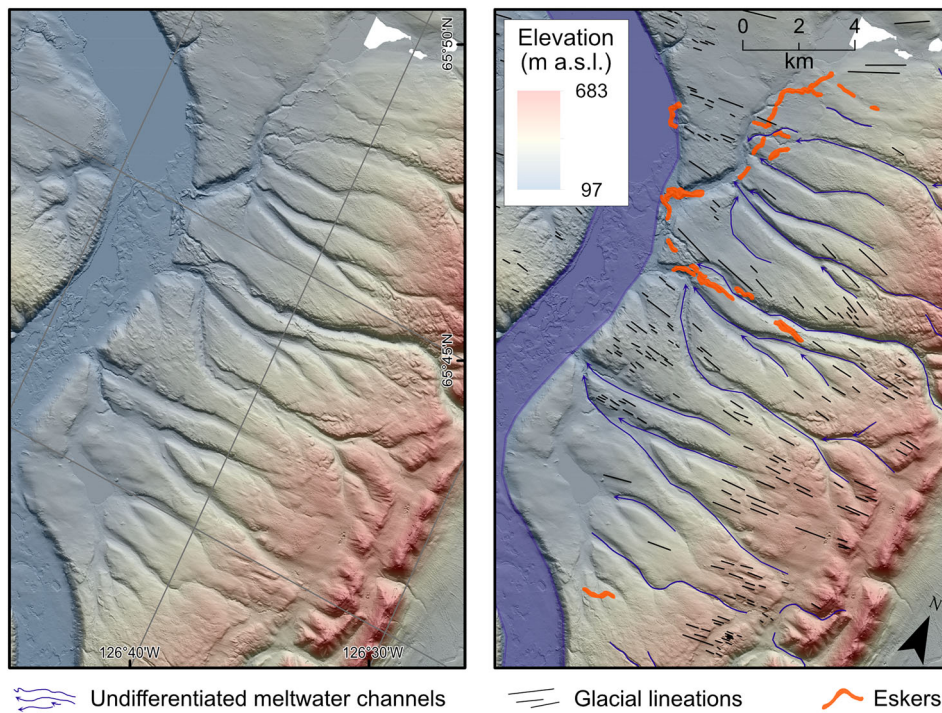


Figure 3. A hillshade image overlain by elevation data from the ArcticDEM showing a series of large subglacial meltwater channels carved into a ridgeline in the Mackenzie Valley. The image location is shown in Figure 1. (a) Subglacial meltwater channels carved through the elevated topography indicate water flow uphill, to the west. The channels are broadly oriented in the same direction as the mapped glacial lineations. A complex esker system is associated with the subglacial channels at the downflow end. (b) The associated geomorphological mapping of glacial landforms.

ranging from simple, single ridges to complex, anabranching esker systems (Figure 5) (cf. Storrar et al., 2015). Eskers are typically oriented subparallel to the former ice flow direction in topographically simple areas (Shreve, 1972; Storrar et al., 2020). These characteristics make them a useful tool for reconstructing the former ice sheet margin retreat patterns in areas of low relief. We mapped eskers as polygons along the break of slope between the landform and the surrounding landscape (Figure 5b).

2.2.4. Moraines

Moraines are linear to arcuate ridges composed of till deposited at the margins of glaciers and ice sheets. They exhibit a variety of morphological forms which reflect the variety of depositional processes which form them (Barr & Lovell, 2014; Chandler et al., 2016; Chandler et al., 2020). Simple moraine forms may include lateral moraines deposited between a glacier and a valley wall which form a single linear ridge, or terminal moraines which form linear to arcuate ridges as sediment accumulates at a glacier terminus. Large hummocky moraines are more complex and may include multiple ridges in a broader zone of chaotic, hummocky terrain. There are a variety of theories about their formation, including the melt-out of stagnant ice to the thrusting of sediment (Eyles et al., 1999; Hambrey et al., 1997). Where available, moraines are an essential tool for reconstructing ice margin retreat

patterns and former ice standstills (Barr & Lovell, 2014). We place moraines into four categories based on the ice source they formed from: Laurentide, Cordilleran, montane, and unknown origin.

We mapped moraines as either polygons or poly-lines depending on their size and morphology (Figure 6). Distinct, individual moraines were mapped as a polyline along the ridge crestline. Larger moraine complexes, hummocky moraines, or multi-ridge moraine complexes were mapped as polygons along the break-of-slope with the surrounding landscape. Distinct moraine ridges visible within hummocky terrain and multi-ridge moraine complexes were also mapped as polylines along the ridge crestline. We recognise that the moraine record in the Mackenzie Mountains region may represent multiple glacial periods (Duk-Rodkin & Hughes, 1992), but we do not attempt to distinguish between moraines of different ages here.

3. Landform distribution

3.1. Glacial lineations

Glacial lineations are widespread across the Mackenzie Mountains region. We map a total of 11,795 glacial lineations, which range from 0.1 km to 10s of km in length. Lination morphology is variable across the study region. In general, lineations mapped within the Mackenzie Valley are more elongate than examples in the Mackenzie Mountains. They are

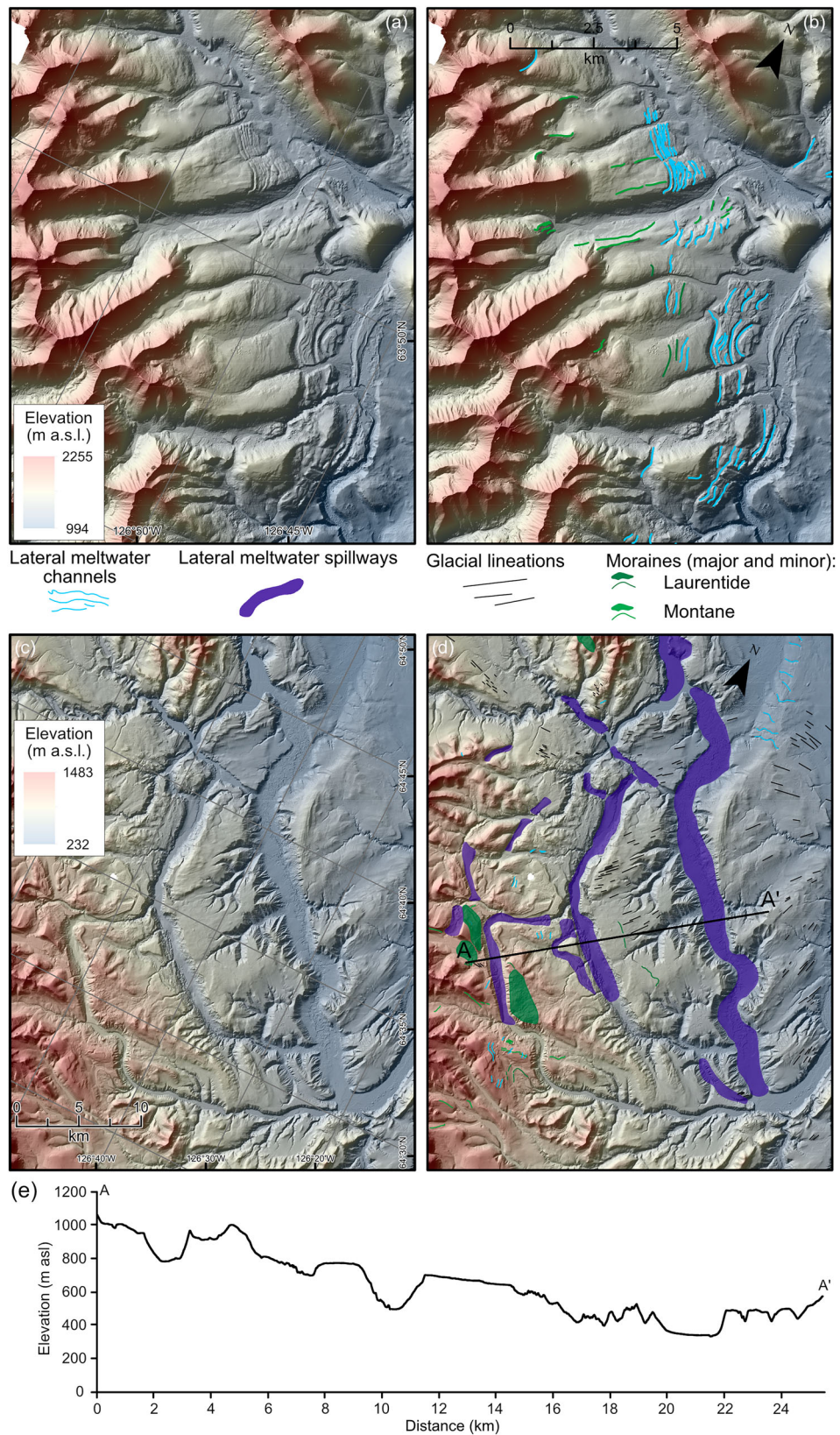


Figure 4. Examples of the range of meltwater channels observed across the study region. Locations are shown in Figure 1. (a) Lateral meltwater channels in the Backbone Ranges of the Mackenzie Mountains, note the cross-cutting relationship with the lateral moraines from nearby montane glaciers. (b) The associated geomorphological mapping of glacial landforms. (c) Lateral meltwater spillways mapped along the eastern slopes of the Mackenzie Mountains. Similar channels are observed all along the eastern range front of the Mackenzie Mountains. (d) The associated geomorphological mapping of glacial landforms. The black line shows the location of a cross-profile highlighting the channel dimensions. (e) Cross-profile of the lateral meltwater spillways.

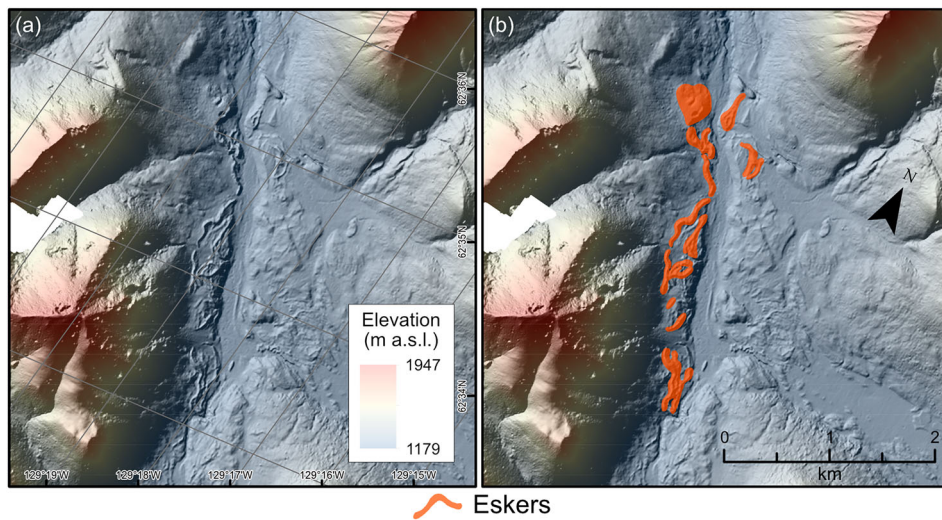


Figure 5. (a) A hillshade image overlain by elevation data from the ArcticDEM showing a complex esker system in the Mackenzie Mountains. (b) The associated geomorphological mapping of glacial landforms. Image location is shown in Figure 1.

most commonly located at lower elevations, in particular, along the valley floors. Almost half of the total glacial lineations (5565) are located in the Mackenzie Valley, associated with the LIS, oriented along the valley profile, in a broadly SE-NW direction. There are some examples which defy this trend, notably in the major valleys of the Mackenzie Mountains, where lineations record the diversion of ice flow up-valley (Main Map). Some high elevation glacial lineations are observed to the south (~1300 m) and the west (~1500–1600 m). Some of the outer summits and ridgelines of the

eastern Mackenzie Mountains also display streamlining from the LIS (~700–800 m around the Carcajou Canyon region), but this is restricted and does not extend far into the mountain range. Our glacial lineation mapping builds upon previous mapping studies. We identify over 3000 lineations in the central Mackenzie Mountains where there are no published surficial geological maps. A major advantage of the ArcticDEM is the ability to more easily discern past ice flow direction. The reconstructed flow directions will provide an insight into the changes in past ice flow dynamics.

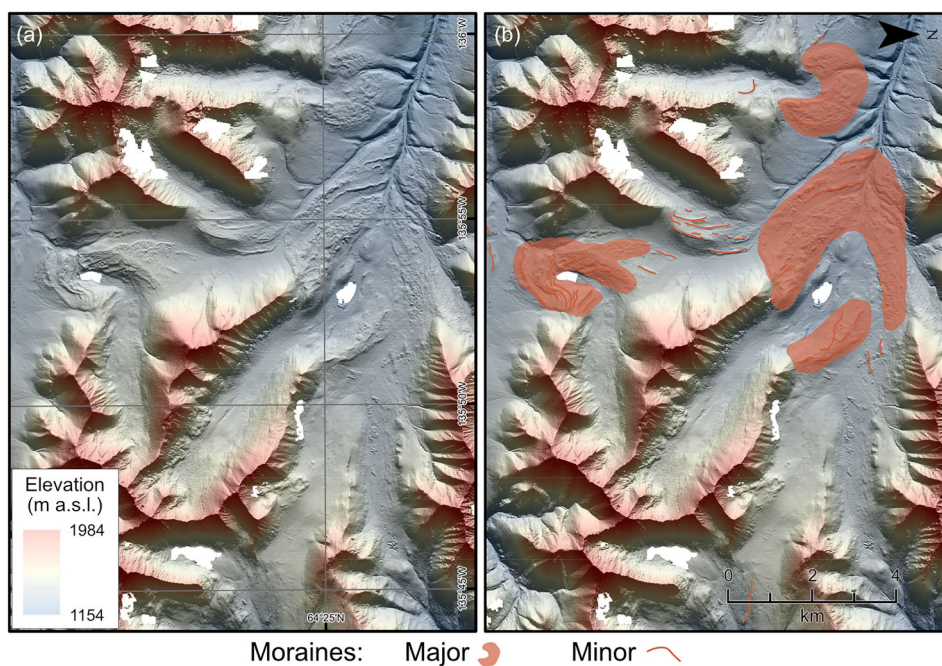


Figure 6. A hillshade image overlain by elevation data from the ArcticDEM showing a series of moraines formed by montane glaciers in the Mackenzie Mountains. Image location is shown in Figure 1. (a) A range of moraine morphologies are observed, including large moraines and more distinct, sharp-crested moraines. (b) The associated geomorphological mapping of glacial landforms.

3.2. Meltwater channels

In total, we mapped 12,862 glacial meltwater channels across the Mackenzie Mountains region, including both undifferentiated meltwater channels ($n = 985$), lateral meltwater channels ($n = 11,805$), and lateral meltwater spillways ($n = 72$).

3.2.1. Lateral meltwater channels

Lateral meltwater channels ($n = 9766$) are extensive across the Mackenzie Mountains region and are the most widespread glaciofluvial feature. The largest concentration of lateral meltwater channels are located in the western Mackenzie Mountains, indicating CIS retreat up valleys to the west ($n = 9227$) (Main Map). Lateral meltwater channels are also carved into the eastern Mackenzie Mountains and on the ridgelines of the Mackenzie Valley associated with the retreat of the LIS (e.g. the Norman Range), but are much less prevalent than the western examples (977) (Figure 4a and b). We also map 778 channels associated with local montane ice masses and 823 meltwater channels of an unknown origin. Over 4000 of these lateral meltwater channels are located in areas of the central and southern Mackenzie Mountains which have not previously been mapped in detail (1:250,000 tiles 95E, 95F, 95L, 95M, 105I, 105P, 106A). Our mapping reproduces the swarms of lateral meltwater channels identified in pre-existing surficial geology maps. However, surficial geology maps based on aerial imagery often map a greater number of lateral meltwater channels in each swarm. This difference would not affect any attempt to reconstruct past ice margin retreat patterns, as our map captures the overall pattern of ice retreat well.

3.2.2. Undifferentiated meltwater channels

We mapped a total of 985 undifferentiated meltwater channels ranging in size from ~ 100 to 10,000 s of metres long. The smaller examples form where a small proglacial lakes dammed between an ice mass and topography flowed over a col. The longer examples formed as the LIS blocked the eastward fluvial drainage. In some cases, this resulted in the drainage being rerouted and north–south drainage networks to be established (Main Map). We identify 150 undifferentiated meltwater channels from areas which have not previously been mapped.

3.2.3. Lateral meltwater spillways

We mapped 72 lateral meltwater spillways which form a discontinuous series of subparallel channels cut across the interfluves of the eastern Mackenzie Mountains, stretching from the Ravens Throat River in the south to the Bonnet Plume Basin in the north (Main Map; Figure 4c, 4d and 4e). These channels have previously been well described and mapped, except those

in the 1:250,000 map tile 95F (Bednarski, 2008a; Duk-Rodkin & Hughes, 1991; Lemmen et al., 1994). They range from 100 to 350 m deep, 400 to 2000 m wide, and are up to 60 km long and so likely carried large volumes of water during deglaciation (Figure 4e).

3.3. Eskers

In total, we mapped 697 eskers across the Mackenzie Mountain region, with a range of complex and simple esker forms observed. Eskers range in size from ~ 0.2 –2 km in length. Longer, more simple esker forms are observed in the Mackenzie Valley compared to the Mackenzie Mountains region (Main Map). This relationship between complex topography and complex eskers is expected as high topographic variability may fragment the drainage system or cause the migration of R-channels in a thin, retreating ice sheet (Stoker et al., 2021; Storrar et al., 2014). Eskers are more commonly located on the valley floors of the Mackenzie Mountains or in the Mackenzie Valley, although some eskers are observed to climb up the topography of broad plateaus in the southern Mackenzie Mountains region. In general, eskers are most common towards the edges of the study area, and are sparse in the central Mackenzie Mountains. Esker orientation is broadly topographically controlled, with ridges oriented subparallel to the valleys they form in. In the Mackenzie Valley, eskers are oriented either SE–NW, subparallel with the valley orientation, with a small amount of eskers oriented W–E across the valley (Main Map). In the Mackenzie Mountains, eskers are more commonly oriented along the valley floor and change orientation to follow the valley, as would be expected for topographically-confined glaciers (Figure 5). While eskers which appear to cross the valley profile or on upland plateaus are less common.

3.4. Moraines

Moraines are most common across the Mackenzie Mountains region ($n = 3939$). The vast majority of moraines were mapped as polylines due to their smaller size ($n = 3810$), compared to larger moraine complexes or hummocky moraines ($n = 129$). These larger moraines, up to 2 km wide and 20 km long, are found along the eastern range front of the Mackenzie Mountains associated with the LIS ($n = 27$) and sporadically in the Backbone Ranges of the Mackenzie Mountains associated with the CIS ($n = 46$) or montane ice masses ($n = 28$) (Figure 6). Smaller moraines are widespread in the central and northern Mackenzie Mountains, typically forming a radial pattern of arcuate ridges around the higher peaks and plateaus, indicating the presence of former icefields (Figure 6). Moraines are cross-cut by meltwater channels in

many locations across the Mackenzie Mountains (Figure 4a and b). In particular, these cross-cutting relationships are observed along the eastern side of the Mackenzie Mountains (Main Map). Our map includes over 1600 moraines within the Mackenzie Mountains region from areas which have not previously been mapped, improving the moraine record in this area. However, our map does not capture the full record of smaller moraines when compared to the pre-existing maps. This is a result of lower quality data, artefacts, and gaps in the ArcticDEM which make it difficult to identify these smaller features in some areas. The record of larger moraines and valley moraines is largely unaffected by these issues.

4. Implications and conclusions

Glaciation of the Mackenzie Mountains region left a geomorphological record marking the maximum extent, changes in ice flow dynamics, and the retreat pattern. We present a glacial geomorphological map based on high-resolution DEM data which updates our knowledge of the glacial geomorphology of the region. Our new map replicates and builds upon pre-existing maps in areas where they are available, providing greater detail for some features (e.g. glacial lineations) and slightly less detail for other features (e.g. meltwater channels), albeit over a larger area. The mapped area also extends into areas where no pre-existing maps are available. The observed cross-cutting relationships in the eastern Mackenzie Mountains are key to deciphering the relative glacial sequence between the ice masses which glaciated the Mackenzie Mountains. The lateral marginal spillways at the eastern range front potentially record valuable information on the drainage of large volumes of meltwater from the LIS along the Mackenzie Mountains during the last deglaciation. This map will underpin future work to create an empirical palaeoglaciological reconstruction of the maximum ice extent, as well as ice flow dynamics and retreat patterns.

Software

The preparation and interpretation of landforms from the ArcticDEM elevation dataset was performed within ESRI ArcGIS v10.6.1, including the creation of hillshades. Landforms were identified and digitised as polylines or polygons in ArcGIS with the Canada Lambert Conformal Conic projection. The map data were exported as SVG files from ArcGIS and used to create the final map panel in Affinity Designer v1.9.

Data

The ESRI shapefiles produced for each glacial landform are provided in the supplementary material to

accompany the paper. This includes both polylines and polygons. The description and classification for each shapefile is contained in the methods section of this paper.

Acknowledgements

We thank Planet Labs who kindly provided free access to high-resolution satellite imagery through the 'Education and Research Program' which we used in this study. This work was supported by funding from the Charles University Grant Agency (GAUK project number 122220) to the lead author (BJS). The area covered by this map includes the territories of multiple First Nations communities in the Northwest Territories and the Yukon and we acknowledge the First Nations people as the traditional owners of these lands. We are grateful for detailed reviews by Dr. Rod Smith and Dr. Jeffrey Bond and for the editorial work of Dr. Brent Ward, which significantly improved the clarity and quality of the manuscript.

Disclosure statement

No potential conflict of interest was reported by the author(s).

Funding

This research was funded by the Charles University Grant Agency (Grantová Agentura, Univerzita Karlova project number 122220).

References

- Barr, I. D., & Lovell, H. (2014). A review of topographic controls on moraine distribution. *Geomorphology*, 226, 44–64. <https://doi.org/10.1016/j.geomorph.2014.07.030>
- Bednarski, J. M. (2008a). Quaternary geology of Fort Liard map area, Northwest Territories. *Geological Survey of Canada, Bulletin*, 596, 59 p. <https://doi.org/10.4095/225608>
- Bednarski, J. M. (2008b). Landform assemblages produced by the Laurentide Ice Sheet in northeastern British Columbia and adjacent Northwest Territories—constraints on glacial lakes and patterns of ice retreat. *Canadian Journal of Earth Sciences*, 45(5), 593–610. <https://doi.org/10.1139/E07-053>
- Boydell, A. N., & Rutter, N. W. (1980). Surficial geology and geomorphology, Root River, District of Mackenzie. *Geological Survey of Canada, Preliminary Map* 12-1979. Scale 1:125,000. <https://doi.org/10.4095/108884>
- Brennand, T. A. (2000). Deglacial meltwater drainage and glaciodynamics: Inferences from Laurentide eskers, Canada. *Geomorphology*, 32(3-4), 263–293. [https://doi.org/10.1016/S0169-555X\(99\)00100-2](https://doi.org/10.1016/S0169-555X(99)00100-2)
- Brown, V. H., Stokes, C. R., & Ó Cofaigh, C. (2011). The glacial geomorphology of the north-west sector of the Laurentide Ice Sheet. *Journal of Maps*, 7(1), 409–428. <https://doi.org/10.4113/jom.2011.1224>
- Chandler, B. M., Evans, D. J. A., & Roberts, D. H. (2016). Characteristics of recessional moraines at a temperate glacier in SE Iceland: Insights into patterns, rates and drivers of glacier retreat. *Quaternary Science Reviews*, 135, 171–205. <https://doi.org/10.1016/j.quascirev.2016.01.025>

- Chandler, B. M., Lovell, H., Boston, C. M., Lukas, S., Barr, I. D., Benediktsson, Í. Ö., Benn, D. I., Clark, C. D., Darvill, C. M., Evans, D. J. A., & Ewertowski, M. W. (2018). Glacial geomorphological mapping: A review of approaches and frameworks for best practice. *Earth-Science Reviews*, 185, 806–846. <https://doi.org/10.1016/j.earscirev.2018.07.015>
- Chandler, B. M., Lukas, S., & Boston, C. M. (2020). Processes of ‘hummocky moraine’ formation in the Gaick, Scotland: Insights into the ice-marginal dynamics of a Younger Dryas plateau icefield. *Boreas*, 49(2), 248–268. <https://doi.org/10.1111/bor.12426>
- Clark, C. D., Tulaczyk, S. M., Stokes, C. R., & Canals, M. (2003). A groove-ploughing theory for the production of mega-scale glacial lineations, and implications for ice-stream mechanics. *Journal of Glaciology*, 49(165), 240–256. <https://doi.org/10.3189/172756503781830719>
- Dalton, A. S., Margold, M., Stokes, C. R., Tarasov, L., Dyke, A. S., Adams, R. S., Allard, S., Arends, H. E., Atkinson, N., Attig, J. W., & Barnett, P. J. (2020). An updated radiocarbon-based ice margin chronology for the last deglaciation of the North American Ice Sheet Complex. *Quaternary Science Reviews*, 234, 106223. <https://doi.org/10.1016/j.quascirev.2020.106223>
- Duk-Rodkin, A. (1999). Glacial limits map of Yukon Territory. *Geological Survey of Canada*, Open File, 3694 (1). Indian and Northern Affairs Canada Geoscience Map 1999-2. Scale 1:1,000,000.
- Duk-Rodkin, A. (2001a). Glacial limits of Wind River, Yukon Territory (106E). *Geological Survey of Canada*, Open File 3795. Scale 1:250,000. <https://doi.org/10.4095/212260>
- Duk-Rodkin, A. (2001b). Glacial limits of Snake River, Yukon Territory (106F). *Geological Survey of Canada*, Open File 3796. Scale 1:250,000. <https://doi.org/10.4095/212261>
- Duk-Rodkin, A. (2001c). Glacial limits of Nash Creek, Yukon Territory (106D). *Geological Survey of Canada*, Open File 3798. Scale 1:250,000. <https://doi.org/10.4095/212263>
- Duk-Rodkin, A. (2001d). Glacial limits of Nadaleen River, Yukon Territory (106C). *Geological Survey of Canada*, Open File 3799. Scale 1:250,000. <https://doi.org/10.4095/212264>
- Duk-Rodkin, A. (2001e). Glacial limits of Bonnet Plume Lake, Yukon Territory (106B). *Geological Survey of Canada*, Open File 3800. Scale 1:250,000. <https://doi.org/10.4095/212266>
- Duk-Rodkin, A. (2001f). Glacial limits of Nidderly Lake-Sekwi Mountain, Yukon Territory (105O&P). *Geological Survey of Canada*, Open File 3803. Scale 1:250,000. <https://doi.org/10.4095/212273>
- Duk-Rodkin, A. (2002). Surficial geology, Norman Wells, Northwest Territories. *Geological Survey of Canada*, “A” Series Map 1989A. Scale 1:250,000. <https://doi.org/10.4095/213617>
- Duk-Rodkin, A. (2005). A GIS dataset of surficial geological features for the Fort Norman map area (96C), Northwest Territories. *Geological Survey of Canada*, Open File 4885. Scale 1:250,000. <https://doi.org/10.4095/220363>
- Duk-Rodkin, A. (2009a). Surficial geology, Dahadinni River (95N/NE), Northwest Territories. *Geological Survey of Canada*, Open File 6060. Scale 1:100,000. <https://doi.org/10.4095/261326>
- Duk-Rodkin, A. (2009b). Surficial geology, Dahadinni River (95N/SE), Northwest Territories. *Geological Survey of Canada*, Open File 6008. Scale 1:100,000. <https://doi.org/10.4095/261324>
- Duk-Rodkin, A. (2018). Surficial geology, Dahadinni River, Northwest Territories, NTS 95-N northwest. *Geological Survey of Canada*, Canadian Geoscience Map 298. Scale 1:100,000. <https://doi.org/10.4095/299113>
- Duk-Rodkin, A. (2022). Glacial limits, Mackenzie Mountains and foothills, Northwest Territories, Canada. *Geological Survey of Canada*, Open File 8891. Scale 1:1,000,000. <https://doi.org/10.4095/10.4095/330011>
- Duk-Rodkin, A., & Barendregt, R. W. (2011). Stratigraphical record of glacial/interglacials in Northwest Canada. *Developments in Quaternary Science*, 15. <https://doi.org/10.1016/B978-0-444-53447-7.00049-0>
- Duk-Rodkin, A., Barendregt, R. W., Froese, D. G., Weber, F., Enkin, R., Smith, I. R., Zazula, G. D., Waters, P., & Klassen, R. (2004). Timing and extent of plio-pleistocene glaciations in north-western Canada and east-central Alaska. *Developments in Quaternary Science*, 2(PART B), 313–345. [https://doi.org/10.1016/S1571-0866\(04\)80206-9](https://doi.org/10.1016/S1571-0866(04)80206-9)
- Duk-Rodkin, A., Barendregt, R. W., Tarnocai, C., & Phillips, F. M. (1996). Late Tertiary to late Quaternary record in the Mackenzie Mountains, Northwest Territories, Canada: Stratigraphy, paleosols, paleomagnetism, and chlorine – 36. *Canadian Journal of Earth Sciences*, 33(6), 875–895. <https://doi.org/10.1139/e96-066>
- Duk-Rodkin, A., & Hughes, O. L. (1991). Age relationships of Laurentide and Montane Glaciations, Mackenzie Mountains, Northwest Territories. *Géographie physique et Quaternaire*, 45(1), 79–90. <https://doi.org/10.7202/032847ar>
- Duk-Rodkin, A., & Hughes, O. L. (1992). Pleistocene Montane Glaciations in the Mackenzie Mountains, Northwest Territories. *Géographie physique et Quaternaire*, 46(1), 69–83. <https://doi.org/10.7202/032889ar>
- Duk-Rodkin, A., & Hughes, O. L. (1993a). Surficial geology, Upper Ramparts River, District of Mackenzie, Northwest Territories. *Geological Survey of Canada*, “A” Series Map 1783A. Scale 1:250,000. <https://doi.org/10.4095/184153>
- Duk-Rodkin, A., & Hughes, O. L. (1993b). Surficial geology, Sans Saule Rapids, District of Mackenzie, Northwest Territories. *Geological Survey of Canada*, “A” Series Map 1784A. Scale 1:250,000. <https://doi.org/10.4095/184008>
- Duk-Rodkin, A., & Hughes, O. L. (1995). Quaternary geology of the northeastern part of the central Mackenzie Valley Corridor, District of Mackenzie, Northwest Territories. *Geological Survey of Canada, Bulletin*, 458. <https://doi.org/10.1017/CBO9781107415324.004>
- Duk-Rodkin, A., & Hughes, O. L. (2002). Surficial geology, Carcajou Canyon, Northwest Territories (096D). *Geological Survey of Canada*, “A” Series Map 1988A. Scale 1:250,000. <https://doi.org/10.4095/213616>
- Duk-Rodkin, A., & Huntley, D. H. (2018a). Surficial geology, Dahadinni River, Northwest Territories, NTS 95-N southwest. *Geological Survey of Canada*, Canadian Geoscience Map 297. Scale 1:100,000. <https://doi.org/10.4095/299112>
- Duk-Rodkin, A., & Huntley, D. H. (2018b). Surficial geology, Root River, Northwest Territories, NTS 95-K northeast. *Geological Survey of Canada*, Canadian Geoscience Map 295. Scale 1:100,000. <https://doi.org/10.4095/299111>
- Dyke, A. S. (1990a). Surficial materials and landforms, Yusezyu River, Yukon Territory. *Geological Survey of Canada*, Map 1676A. Scale 1:100,000. <https://doi.org/10.4095/130938>
- Dyke, A. S. (1990b). Surficial materials and landforms, Little Hyland River, Yukon Territory. *Geological Survey of*

- Canada, Map 1677A. Scale 1:100,000. <https://doi.org/10.4095/130939>
- Dyke, A. S. (1990c). Surficial materials and landforms, Frances River, Yukon Territory. *Geological Survey of Canada*, Map 1675A. Scale 1:100,000. <https://doi.org/10.4095/130937>
- Dyke, A. S. (1990d). Surficial materials and landforms, Dolly Varden Creek, Yukon Territory. *Geological Survey of Canada*, Map 1674A. Scale 1:100,000. <https://doi.org/10.4095/130936>
- Dyke, A. S., Moore, A., & Robertson, L. (2003). Deglaciation of North America. *Geological Survey of Canada*, Open File, 1574. <https://doi.org/10.4095/214399>
- Ely, J. C., Clark, C. D., Spagnolo, M., Stokes, C. R., Greenwood, S. L., Hughes, A. L., Dunlop, P., & Hess, D. (2016). Do subglacial bedforms comprise a size and shape continuum? *Geomorphology*, 257, 108–119. <https://doi.org/10.1016/j.geomorph.2016.01.001>
- Eyles, N., Boyce, J. I., & Barendregt, R. W. (1999). Hummocky moraine: sedimentary record of stagnant Laurentide Ice Sheet lobes resting on soft beds. *Sedimentary Geology*, 123(3-4), 163–174. [https://doi.org/10.1016/S0037-0738\(98\)00129-8](https://doi.org/10.1016/S0037-0738(98)00129-8)
- Eyles, N., Putkinen, N., Sookhan, S., & Arbelaez-Moreno, L. (2016). Erosional origin of drumlins and megaridges. *Sedimentary Geology*, 338, 2–23. <https://doi.org/10.1016/j.sedgeo.2016.01.006>
- Fowler, A. C. (2000). An instability mechanism for drumlin formation. *Geological Society, London, Special Publications*, 176(1), 307–319. <https://doi.org/10.1144/GSL.SP.2000.176.01.23>
- Gomez, N., Gregoire, L. J., Mitrovica, J. X., & Payne, A. J. (2015). Laurentide-Cordilleran ice sheet saddle collapse as a contribution to meltwater pulse 1A. *Geophysical Research Letters*, 42(10), 3954–3962. <https://doi.org/10.1002/2015GL063960>
- Greenwood, S. L., Clark, C. D., & Hughes, A. L. (2007). Formalising an inversion methodology for reconstructing ice-sheet retreat patterns from meltwater channels: Application to the British Ice Sheet. *Journal of Quaternary Science*, Published for the Quaternary Research Association, 22(6), 637–645. <https://doi.org/10.1002/jqs.1083>
- Gregoire, L. J., Otto-Bliesner, B., Valdes, P. J., & Ivanovic, R. (2016). Abrupt Bølling warming and ice saddle collapse contributions to the Meltwater Pulse 1a rapid sea level rise. *Geophysical Research Letters*, 43(17), 9130–9137. <https://doi.org/10.1002/2016GL070356>
- Gregoire, L. J., Payne, A. J., & Valdes, P. J. (2012). Deglacial rapid sea level rises caused by ice-sheet saddle collapses. *Nature*, 487(7406), 219–222. <https://doi.org/10.1038/nature11257>
- Hambrey, M. J., Huddart, D., Bennett, M. R., & Glasser, N. F. (1997). Genesis of ‘hummocky moraines’ by thrusting in glacier ice: Evidence from Svalbard and Britain. *Journal of the Geological Society*, 154(4), 623–632. <https://doi.org/10.1144/gsjgs.154.4.0623>
- Hart, J. K., Clayton, A. I., Martinez, K., & Robson, B. A. (2018). Erosional and depositional subglacial streamlining processes at Skálafellsjökull, Iceland: An analogue for a new bedform continuum model. *Gff*, 140(2), 153–169. <https://doi.org/10.1080/11035897.2018.1477830>
- Jackson, L. E., Andriashek, L. D., & Phillips, F. M. (2011). Limits of successive Middle and Late Pleistocene continental ice sheets, interior plains of southern and central Alberta and adjacent areas. In *Developments in Quaternary sciences* (Vol. 15, pp. 575–589). Elsevier. <https://doi.org/10.1016/B978-0-444-53447-7.00045-3>
- King, E. C., Hindmarsh, R. C., & Stokes, C. R. (2009). Formation of mega-scale glacial lineations observed beneath a West Antarctic ice stream. *Nature Geoscience*, 2(8), 585–588. <https://doi.org/10.1038/ngeo581>
- Kleman, J. (1992). The palimpsest glacial landscape in north-western Sweden: Late Weichselian deglaciation landforms and traces of older west-centered ice sheets. *Geografiska Annaler: Series A, Physical Geography*, 74(4), 305–325. <https://doi.org/10.1080/04353676.1992.11880373>
- Lemmen, D. S., Duk-Rodkin, A., & Bednarski, J. M. (1994). Late glacial drainage systems along the northwestern margin of the Laurentide Ice Sheet. *Quaternary Science Reviews*, 13(9–10), 805–828. [https://doi.org/10.1016/0277-3791\(94\)90003-5](https://doi.org/10.1016/0277-3791(94)90003-5)
- Margold, M., & Jansson, K. N. (2012). Evaluation of data sources for mapping glacial meltwater features. *International Journal of Remote Sensing*, 33(8), 2355–2377. <https://doi.org/10.1080/01431161.2011.608738>
- Margold, M., Jansson, K. N., Kleman, J., & Stroeven, A. P. (2013). Lateglacial ice dynamics of the Cordilleran Ice Sheet in northern British Columbia and southern Yukon Territory: retreat pattern of the Liard Lobe reconstructed from the glacial landform record. *Journal of Quaternary Science*, 28(2), 180–188. <https://doi.org/10.1002/jqs.2604>
- Matthews, W. H. (1980). Retreat of the last ice sheets in northeastern British Columbia and adjacent Alberta. *Geological Survey of Canada, Bulletin*, 331, 22 pages. <https://doi.org/10.4095/102160>
- Menounos, B., Goehring, B. M., Osborn, G., Margold, M., Ward, B., Bond, J., Clarke, G. K., Clague, J. J., Lakeman, T., Koch, J., & Caffee, M. W. (2017). Cordilleran Ice Sheet mass loss preceded climate reversals near the Pleistocene Termination. *Science*, 358(6364), 781–784. <https://doi.org/10.1126/science.aan3001>
- Möller, P., & Dowling, T. P. (2018). Equifinality in glacial geomorphology: Instability theory examined via ribbed moraine and drumlins in Sweden. *GFF*, 140(2), 106–135. <https://doi.org/10.1080/11035897.2018.1441903>
- Ó Cofaigh, C. (1996). Tunnel valley genesis. *Progress in Physical Geography: Earth and Environment*, 20(1), 1–19. <https://doi.org/10.1177/030913339602000101>
- Planet Team. (2018). *Planet application program interface: In space for life on earth*. San Francisco, CA. <https://api.planet.com>
- Porter, C., Morin, P., Howat, I., Noh, M.-J., Bates, B., Peterman, K., Keeseey, S., Schlenk, M., Gardiner, J., Tomko, K., Willis, M., Kelleher, C., Cloutier, M., Husby, E., Foga, S., Nakamura, H., Platson, M., Wethington, M., Williamson, C., ... Bojesen, M. (2018). “ArcticDEM”. Retrieved May 28, 2021, from <https://doi.org/10.7910/DVN/OHHUKH>, Harvard Dataverse, V1
- Rutter, N. W., Hawes, R. J., & Catto, N. R. (1993). Surficial geology, southern Mackenzie River valley. District of Mackenzie, Northwest Territories. *Geological Survey of Canada*, Map 1693a. Scale 1:500,000. <https://doi.org/10.4095/193343>
- Shaw, J., Sharpe, D., & Harris, J. (2010a). A flowline map of glaciated Canada based on remote sensing data. *Canadian Journal of Earth Sciences*, 47(1), 89–101. <https://doi.org/10.1139/E09-068>
- Shaw, J., Sharpe, D. R., Harris, J. R., Lemkow, D., & Pehleman, D. (2010b). Digital landform patterns for glaciated regions of Canada—a predictive model of flow lines based on topographic and LANDSAT 7 data. *Geological Survey of Canada*, Open File, 5745. <https://doi.org/10.4095/286248>

- Shreve, R. L. (1972). Movement of water in glaciers. *Journal of Glaciology*, 11(62), 205–214. <https://doi.org/10.3189/S002214300002219X>
- Smith, I. R. (2003a). Surficial geology Babiche Mountain (95C/8), Northwest Territories – Yukon Territory. *Geological Survey of Canada*, Open File 1558. Scale 1:50 000. <https://doi.org/10.4095/214147>
- Smith, I. R. (2003b). Surficial geology Etanda Lakes (95C/16), Northwest Territories – Yukon Territory. *Geological Survey of Canada*, Open File 1671. Scale 1:50 000. <https://doi.org/10.4095/214291>
- Smith, M. J., & Clark, C. D. (2005). Methods for the visualization of digital elevation models for landform mapping. *Earth Surface Processes and Landforms*, 30(7), 885–900. <https://doi.org/10.1002/esp.1210>
- Stoker, B. J., Livingstone, S. J., Barr, I. D., Ruffell, A., Storrar, R. D., & Roberson, S. (2021). Variations in esker morphology and internal architecture record time-transgressive deposition during ice margin retreat in Northern Ireland. *Proceedings of the Geologists' Association*, 132(4), 409–425. <https://doi.org/10.1016/j.pgeola.2021.03.002>
- Stoker, B. J., Margold, M., Gosse, J. C., Hidy, A. J., Monteath, A. J., Young, J. M., Gandy, N., Gregoire, L. J., Norris, S. L., & Froese, D. (2022). The collapse of the Cordilleran–Laurentide ice saddle and early opening of the Mackenzie Valley, Northwest Territories, Canada, constrained by 10 Be exposure dating. *The Cryosphere*, 16(12), 4865–4886. <https://doi.org/10.5194/tc-16-4865-2022>
- Stokes, C. R., & Clark, C. D. (2002). Are long subglacial bedforms indicative of fast ice flow? *Boreas*, 31(3), 239–249. <https://doi.org/10.1080/030094802760260355>
- Stokes, C. R., Fowler, A. C., Clark, C. D., Hindmarsh, R. C., & Spagnolo, M. (2013). The instability theory of drumlin formation and its explanation of their varied composition and internal structure. *Quaternary Science Reviews*, 62, 77–96. <https://doi.org/10.1016/j.quascirev.2012.11.011>
- Storrar, R. D., Evans, D. J. A., Stokes, C. R., & Ewertowski, M. (2015). Controls on the location, morphology and evolution of complex esker systems at decadal timescales, Breidamerkurjökull, southeast Iceland. *Earth Surface Processes and Landforms*, 40(11), 1421–1438. <https://doi.org/10.1002/esp.3725>
- Storrar, R. D., Ewertowski, M., Tomczyk, A. M., Barr, I. D., Livingstone, S. J., Ruffell, A., Stoker, B. J., & Evans, D. J. A. (2020). Equifinality and preservation potential of complex eskers. *Boreas*, 49(1), 211–231. <https://doi.org/10.1111/bor.12414>
- Storrar, R. D., Stokes, C. R., & Evans, D. J. A. (2014). Morphometry and pattern of a large sample (> 20,000) of Canadian eskers and implications for subglacial drainage beneath ice sheets. *Quaternary Science Reviews*, 105, 1–25. <https://doi.org/10.1016/j.quascirev.2014.09.013>
- Sugden, D. E., Denton, G. H., & Marchant, D. R. (1991). Subglacial meltwater channel systems and ice sheet overriding, Asgard Range, Antarctica. *Geografiska Annaler: Series A, Physical Geography*, 73(2), 109–121. <https://doi.org/10.1080/04353676.1991.11880335>
- Trommelen, M., & Levson, V. (2008). Quaternary stratigraphy of the Prophet River, northeastern British Columbia. *Canadian Journal of Earth Sciences*, 45(5), 565–575. <https://doi.org/10.1139/E07-072>
- Turner, D. G., Ward, B., & Bond, J. D. (2008a). Glacial history of Howard's pass and applications to drift prospecting. *Yukon Exploration and Geology*, 257–272. https://emrlibrary.gov.yk.ca/ygs/yeg/2007/2007_p257-272.pdf
- Turner, D. G., Ward, B. C., & Bond, J. D. (2008b). Surficial Geology of the Howard's Pass area (NTS 105I/12 and parts of 105I/11, 6 and 5 and 105J/9 and 8), Yukon and Northwest Territories. Yukon Geological Survey, Open File 2008-19.
- Zazula, G. D., Duk-Rodkin, A., Schweger, C. E., & Morlan, R. E. (2004). Late Pleistocene chronology of glacial Lake Old Crow and the north-west margin of the Laurentide Ice Sheet. In J. Ehlers & P. L. Gibbard (Eds.), *Developments in quaternary sciences* (Vol. 2, pp. 347–362). Elsevier. [https://doi.org/10.1016/S1571-0866\(04\)80207-0](https://doi.org/10.1016/S1571-0866(04)80207-0)